Physics Letters B 790 (2019) 102–107

Contents lists available at ScienceDirect

Physics Letters B

www.elsevier.com/locate/physletb

Heavy quark mass effects in parton-to-kaon hadronization probabilities

Manuel Epele [a], Carlos García Canal [a], R. Sassot [b]

[a] Instituto de Física La Plata, UNLP, CONICET, Departamento de Física, Facultad de Ciencias Exactas, Universidad de La Plata, C.C. 69, La Plata, Argentina
[b] Departamento de Física and IFIBA, Facultad de Ciencias Exactas y Naturales, Universidad de Buenos Aires, Ciudad Universitaria, Pabellón 1 (1428) Buenos Aires, Argentina

ARTICLE INFO

Article history:
Received 20 July 2018
Received in revised form 22 November 2018
Accepted 26 November 2018
Available online 28 December 2018
Editor: M. Doser

ABSTRACT

We examine the relevance of the heavy quarks masses in the perturbative QCD description of hard interactions where charged kaons are produced in the final state. We extract a set of parton-to-kaon hadronization probabilities from a next to leading order QCD global analysis where a general mass variable flavor number scheme accounting for mass effects is implemented. We compare the results with those obtained in the massless approximation and also with those found in the case of final state pions. At variance with the very significant improvement found for the much more precise pion fragmentation phenomenology, the heavy quark mass dependent scheme improves mildly the overall description of current kaon production data. Nevertheless, we find a noticeable reduction in the charm-to-kaon hadronization probability.

1. Introduction

Ultra-relativistic proton–proton collisions produce very large numbers of final particles, some of which emerge with transverse momentum of several GeV. The most sought signals, those whose behavior deviates from our present paradigm and that could indicate novel physical phenomena, are expected to be hidden beneath ordinary events which constitute an overwhelming background. The largest fraction of this background in experiments such as those performed at the Large Hadron Collider [1] and at the Relativistic Heavy Ion Collider [2] are light hadrons, such as pions and kaons. These are produced in the final state through the hadronization or fragmentation mechanism by which hard interacting partons evolve into a physical and intrinsically non-perturbative colorless hadronic state. In the context of perturbative Quantum Chromodynamics (QCD) [3], hard hadronic collisions with identified final state hadrons are described perturbatively in terms of effective hard scattering cross sections and two sets of universal non-perturbative functions: parton distributions (PDF), which describe the internal structure of the hadrons just before the interaction process, and fragmentation functions (FF) that encode the information about the hadronization processes [4].

Because of their non perturbative nature, PDFs and FFs need to be extracted through QCD global analyses of experimental data, where the hard scattering cross sections are approximated with increasing precision [5,6]. The first generations of these global analyses relied on the massless quark approximations of QCD but progressively, a growing interest has been focussed in how the non-perturbative distributions are affected by considering quarks as massive particles. Of course, the relevance of dynamical effects associated to the quarks masses in a hard interaction depends crucially on both the masses and the energy scale that characterizes the process. For *up*, *down* and *strange* quarks, the same restriction that allows a perturbative treatment, i.e. energy scales much larger than $\Lambda_{\rm QCD}$, guarantees the smallness of potential dynamical effects arising from their masses, making natural to treat them as massless, with the advantage of the all-order resummations implicit in massless parton approaches. However, this is not the case for charm and bottom quarks, whose mass thresholds fall inside the perturbative domain and produce the corresponding dynamical signatures and consequently need all-order resummations at very high energy scales. The so called general mass factorization schemes with a variable number of flavors (GMVFN) reproduce accurately both the massive and the massless regimes, smoothly interpolating between them [7].

In the case of PDFs, the implementation of different variants of a GMVFN factorization scheme has become the standard practice to include heavy quark mass effects, keeping the consistency to the

E-mail addresses: manuepele@fisica.unlp.edu.ar (M. Epele), garcia@fisica.unlp.edu.ar (C. García Canal), sassot@df.uba.ar (R. Sassot).

https://doi.org/10.1016/j.physletb.2018.11.069

high energy limit [5]. The strategy devised for PDFs can be adapted to account for heavy quark mass effects in FFs extractions. Indeed, different schemes have already been applied to assess heavy quark hadronization probabilities into heavy flavored hadrons [8]. More recently, a GMVFN scheme, based on the FONLL scheme [9,10] and aimed to improve the precision in parton-to-pion FFs, was successfully implemented in a QCD global analysis [11]. The mass dependent picture introduced by a GMVFN scheme was shown to modify significantly the hadronization probabilities of charm quarks into pions, due to the retention of the hard scattering mass effects in the partonic cross sections, rather than factorizing them into the FFs, in a consistent way. Additionally, the approach improves the quality of the fit to data, especially for data standing closer to the heavy quarks mass thresholds, and reduces the normalization shifts customarily included to accommodate data sets in the analysis [12].

In the following we implement the GMVFN scheme in a global analysis designed to extract parton-to-kaon FFs. As it was done in the case of pion FFs, the dynamic effects related to the heavy quarks masses are computed up to next to leading order (NLO) in perturbation for the single inclusive electron–positron annihilation (SIA) cross section. In the next section, we discuss very briefly kaon fragmentation and the role of heavy quarks in it. Then, we sketch how the GMVFN scheme is implemented within the complex Mellin moment technique in a global fit to current data in an efficient way, and show the corresponding results. We find a sizeable modification of the shape of the charm-to-kaon fragmentation function compared to the one obtained from the massless QCD approximation. The bottom fragmentation is found to be similar to the one obtained in the massless approximation, as it is constrained mostly by data well above the bottom mass production threshold, where mass effects are suppressed. At variance with the analysis performed using much more precise pion production data, we see only a mild improvement in the quality of the fit.

2. Heavy quark into kaon fragmentation

First efforts to determine light hadron FFs through next-to-leading order (NLO) QCD analyses [13,14] typically focussed on very precise electron–positron annihilation data collected at LEP and SLAC, at energy scales close to the Z-boson mass, that is roughly twenty times larger than the bottom mass. To reproduce these data, a massless approach for the parton dynamics at first sight is a sensible approximation. Even extending SIA only studies to true global analyses, where extra information coming from hadron production in semi-inclusive deeply inelastic scattering (SIDIS) and in proton–proton (pp) collisions at much lower energy scales is used as a complement, the approximation seems still justified. In these additional processes, the contributions triggered by heavy flavor are strongly suppressed, hidden among many other contributions related to sea quarks in the initial state protons.

Nevertheless, global analyses based on the massless perturbative QCD approximation, show that the non-perturbative hadronization probabilities for heavy quarks into light hadrons are, themselves, not negligible at all [14]. Notice that within the QCD factorization approach, fragmentation functions are associated to the description of processes where the hadron observed in the final state is produced immediately after the hard interaction that excites the heavy quarks, but not those produced as secondary decays of other intermediate heavy hadrons. These fragmentation probabilities are of nonperturbative nature and can not be computed from first principles within perturbation theory, neither can be visualized or represented by partonic interactions for the same reason. But they can be extracted from the data, factorizing in

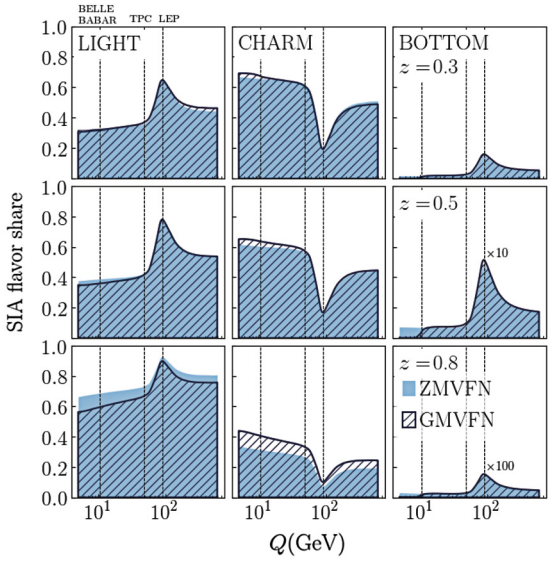

Fig. 1. Comparison between the relative contributions of light, charm and bottom flavor hadronization to the total single-kaon production cross section in electron–positron annihilation processes computed with the ZMVFN and GMVFN schemes as a function of the energy scale Q.

the measured cross section the hard, short distance, component. Indeed, they are found to be as large in size as valence quark hadronization probabilities, and they contribute to a significant fraction of the SIA cross section [3,6]. Indeed, they may be as large in size as valence quark hadronization probabilities, and they contribute to a significant fraction of the SIA cross section. In order to illustrate this point, in Fig. 1 we show the fraction of the charged kaon SIA cross section contributed by light, charm and bottom quark fragmentation, respectively, as a function of the energy scale and in three different hadron momentum fraction regions. The colored areas represent the results coming from a typical zero mass variable flavor number scheme (ZMVFN) analysis like the DSS07 [14] or DSS17 [15] NLO sets, but with slightly updated inputs that will be specified in the next section. In the ZMVFN schemes, cross sections are computed in the massless approximation, however the charm and bottom contributions start only after the hard scale becomes larger than the respective heavy quark mass threshold. Below the Z-boson mass scale, and for kaons carrying a not very large fraction ($z < 0.6$) of the total available center of mass energy, charm quark fragmentation dominates the SIA cross section. This dominant charm contribution comes in part from the size of the charm FF itself, comparable to the total *strange* FF, but that enters the SIA cross section multiplied by a four times larger electroweak charge factor, and that is also three times bigger than the total *up* FF. Approaching the Z-boson mass scale, the electroweak charge suppress the relative charm contribution. For increasing kaon energy fractions, one recovers a more intuitive picture, where *strange* and *up* quark fragmentation dominates the SIA cross section. On the other hand, the bottom FF is found to be much smaller than the one for charm, and combined with the also smaller charge factor, produces a very minor contribution. Anticipating the results from the GMVFN scheme, the dashed areas show the same but estimated with FFs obtained keeping mass effects, and will be discussed in detail later.

In addition to the typical size of the charm quark contribution to the SIA cross section, if a set of SIA data sits close to the mass thresholds, then the mass effects are no longer suppressed and consequently are expected to become relevant in the flavor separation. Mass effects would have a direct impact in the charm quark FF through the SIA cross section coefficients and also an indirect

effect in the gluon FF through its evolution to high energies, since it is coupled to the charm. In fact, in the last decade there has been a substantial improvement in the precision of hadron production measurements at relatively low energy scales such as Belle [17] and BaBar [16] experiments, rising the question of how necessary is it to improve the description of hadronization processes including the dynamics of heavy quarks to match their precision.

3. GMVFN scheme global analysis

The most simple way to account for the dynamical effects associated to the heavy quark masses consists in the implementation of factorization schemes with a fixed number of flavors (FFNS). In these schemes, the partonic cross sections are computed retaining the mass dependent terms and the number of active flavors is defined by the energy scale of the process to be described. These schemes are appropriate to reproduce hard interaction processes at energy scales close to the heavy flavor masses, however, they are not adequate to handle multiple energy scale problems, like a QCD global analysis. The limitation comes precisely from treating heavy quarks as massive particles always, what leads to some potentially dangerous logarithmic contributions in the partonic cross sections when the energy scale becomes much larger than the mass scales. Such logarithmic contributions may spoil the accuracy of perturbative calculations.

In the opposite scenario, in the renormalization group improved massless quark approach, a process independent resummation of the logarithmic contributions deals with the problem at high energies, but gives an obviously inadequate description close to the mass thresholds. The general mass variable flavor number scheme (GMVFN) is designed to interpolate continuously and smoothly between the low energy regime, where the heavy quarks are treated as massive particles, and the high energy one, where the dynamic effects of all parton masses are negligible. In this way, the dynamics of heavy quarks are consistently described across the entire range of energy scales relevant for a QCD global analysis. As for any factorization scheme, the definition of GMVFN scheme is not unique. There is a certain degree of arbitrariness that reflects in how fast the massive picture converges to the massless limit [11]. This particular feature of the approach, rather than a weakness, can be exploited to optimize the description of data.

The implementation of a GMVFN scheme in a QCD global analysis for FFs has already been discussed in detail in the case of pion FFs in [11]. The main point is that appropriately subtracted massive cross sections are convoluted with the parametrizations of the corresponding fragmentation functions, evolved through the standard DGLAP evolution equations [18]. The unknown parameters, that define the hadronization probabilities, are determined as usual by comparing experimental measurements and their theoretical predictions, through a suitable χ^2 function:

$$\chi^2 = \sum_{i=1}^{N} \left[\left(\frac{1-\mathcal{N}_i}{\delta \mathcal{N}_i} \right)^2 + \sum_{j=1}^{N_i} \frac{(\mathcal{N}_i T_j - E_j)^2}{\delta E_j^2} \right], \tag{1}$$

here $i = 1, \ldots, N$ labels the data sets, each contributing with N_i data points. E_j is the measured value for a given observable, δE_j the error associated with this measurement, and T_j is the corresponding theoretical estimate for a given set of parameters. Since the full error correlation matrices are not available for some of the data sets used in the fit, statistical and systematical errors are simply added in quadrature in δE_j as in previous fits [12,14,15]. Normalization shifts $\mathcal{N}_i$, introduced for each data set to account for the quoted normalization uncertainties are computed analytically from the condition $\partial \chi^2 / \partial \mathcal{N}_i = 0$ in each iteration, with a corresponding penalty.

The Mellin moment approach is used to perform all the calculations required for the parameter determination in an efficient way [14]. This technique allows to replace the convolution integrals required by the computation of cross sections and also those for the evolution equations of the FFs at the initial scale where they are parameterized by simple products. Because of the complexity of the mass dependent expressions inherent to the GMVFN partonic cross sections, it is helpful to numerically compute their Mellin transforms and tabulate them before the global fit is performed. To recover the cross sections in the z-space, Mellin inversion integrals require the use of appropriate contours in the line integrals in complex moment space as described in [19]. As in ref. [11], the specific prescription for the GMVFN scheme is chosen in order to optimize the description of the complete set of experimental data included in the global analysis. We found that the same prescription as in the case of pions, suggesting that the preference for a faster or slower convergence to the massless limit could be universal, is related to the heavy quarks dynamics rather than to the final state hadron species.

The SIA-to-parton cross sections were computed at NLO in perturbation theory retaining charm quark and bottom quark masses in the framework of a GMVFN scheme. From the point of view of the perturbative QCD framework, the most consistent choice would be to consider data on primary hadrons or decay products with the shortest possible lifetimes. In our analysis, we use subtracted (Belle) or prompt data (BaBar) when available to reduce as much as possible the secondary decays, as it is customary in other extractions. The value for the running strong coupling α_s is the one obtained in the NLO NNPDF3.0 extraction of PDFs [20] ($\alpha_s(M_z) = 0.118$) that implements also a GMVFN factorization scheme. We also adopt their convention for heavy quark masses, i.e. pole masses and $m_c = 1.275$ GeV, $m_b = 4.18$ GeV, for charm and bottom, respectively. Hadroproduction cross sections in proton–proton collisions and SIDIS are computed with this PDF set, but in the massless parton approximation, since for these particular processes heavy quark contributions are strongly suppressed relative to the lighter flavors. The use of these PDFs has been shown to give a much better description of SIDIS data than other PDF sets [29]. As in previous extractions [14,15], in order to compute the hadroproduction cross sections in proton–proton collisions we set the factorization and renormalization scales to be equal to the observed hadron transverse momentum. The transverse momentum range of the STAR data from Ref. [24] included in the fit is 5–13 GeV at 200 GeV, and 5–13 GeV for ALICE at 2.76 TeV. The scale and PDF uncertainties with the NNPDF3.0 sets are similar to those found with other modern sets of PDFs and quite large for cross section, see Refs. [12,30] for estimates, but they tend to cancel taking cross section ratios. They were included in the χ^2 minimization adding them in quadrature to the experimental error.

At variance with the pion SIA data, the kaon production cross section measured by BABAR collaboration at 10.54 GeV, is about a 10% larger than the one measured by the BELLE experiment at 10.52 GeV in most of the kaon energy fraction range ($0.3 < z < 0.8$). This difference is significantly larger than the normalization uncertainties estimated by both collaborations. Different strategies to estimate and subtract kaons from secondary decays in both experiments, for example, could contribute to such differences. In any case, a full analysis of the origin of this feature is beyond the scope of the present analysis. In ref. [15], the apparent difference between both data sets was treated as a typical normalization error and absorbed into the normalization shifts $\mathcal{N}_i$ introduced in Eq. (1). In consequence, the fit to data negotiate an intermediate solution that reproduce neither of the data sets. Alternatively, one could assume the difference between both ex-

Table 1
Individual χ^2 contributions and normalization shifts $\mathcal{N}_i$ obtained analytically from Eq. (1) for the data sets included in two global analyses where the ZMVFN and GMVFN schemes have been implemented. In the case of BaBar data, there is an extra 10% fixed normalization shift not included in $\mathcal{N}_i$, as explained in the text.

Experiment	Data type	# data in fit	ZMVFN		GMVFN	
			$\mathcal{N}_i$	χ^2	$\mathcal{N}_i$	χ^2
ALEPH [21]	incl.	13	1.011	8.6	1.023	7.6
BABAR [16]	incl.	30	1.065	24.4	1.005	10.4
BELLE [17]	incl.	78	0.983	16.5	1.009	14.7
DELPHI [22]	incl.	12	1.000	7.8	1.000	5.3
	uds tag	12	1.000	7.9	1.000	8.1
	b tag	12	1.000	4.0	1.000	2.8
SLD [23]	incl.	18	1.002	8.0	1.005	7.4
	uds tag	10	1.002	13.3	1.005	12.3
	c tag	10	1.002	19.1	1.005	17.7
	b tag	10	1.002	11.6	1.005	11.8
TPC [24]	incl. 34 GeV	4	1.000	1.8	1.000	1.9
TPC [24]	incl. 29 GeV	12	1.000	12.2	1.000	10.0
COMPASS [25]	K^+(d)	309	1.012	229.2	1.013	229.4
	K^-(d)	309	1.012	211.8	1.013	209.5
HERMES [26]	K^+(p) Q^2	36	0.830	62.6	0.832	61.2
	K^-(p) Q^2	36	0.830	34.2	0.832	34.0
	K^+(p) x	36	1.124	69.1	1.127	69.0
	K^-(p) x	36	1.124	35.1	1.127	35.7
	K^+(d) Q^2	36	0.836	41.8	0.838	41.0
	K^-(d) Q^2	36	0.836	36.2	0.838	35.7
	K^+(d) x	36	1.091	38.3	1.094	38.5
	K^-(d) x	36	1.091	32.0	1.094	32.2
STAR [27]	K^+, K^+/K^-	16	1.085	7.6	1.085	7.5
ALICE [28]	K/π	15	0.991	11.7	0.992	11.0
TOTAL:		1158		944.8		913.9

periments as coming from two differently defined observables, and let the minimization decide which definition suits best the rest of data in the fit, shifting the second so that both data sets agree. Doing this, we find a much better overall agreement between data and theory shifting down by around a 10% the BABAR data set. Another possibility would be to consider that the data sets are not compatible and eliminate one of them from the fit, retaining the one that leads to best overall agreement. However, we find that this latter approach leads basically to the same result as in the previous alternative.

In Table 1 we present the results of two analyses implementing ZMVFN and the GMVFN schemes, respectively, indicating the partial contributions to χ^2 and normalizations for each of the data sets included in the fit. As it can be noticed, most of the SIA data sets are slightly better described in the GMVFN framework and with typically smaller normalization shifts. The effect is particularly noticeable for BABAR and BELLE with a reduction from 6.5 to 0.6 %, and 1.7 to 0.9 % respectively. Notice that the additional normalization applied to BABAR data discussed in the previous paragraph and motivated by a direct comparison between the two data sets at roughly the same center of mass energies, is implemented in both the ZMVFN and the GMVFN analyses. The improvement leading to smaller values for $\mathcal{N}_i$ is a direct consequence of the GMVFN scheme, since it induces a slightly different z-dependence in the SIA cross section that fits better the data, and further reduces the tension with other data sets at different energies.

In a previous QCD global analyses performed within the ZMVFN scheme [15], the exclusion of the bottom channel in the estimate of the SIA kaon production cross section at low center of mass energy scale was necessary to reproduce BELLE and BABAR measurements. In the GMVFN scheme, this contribution is highly suppressed near the $2m_b$ threshold, and in consequence the whole data included in the global fit is described in a much more natural way.

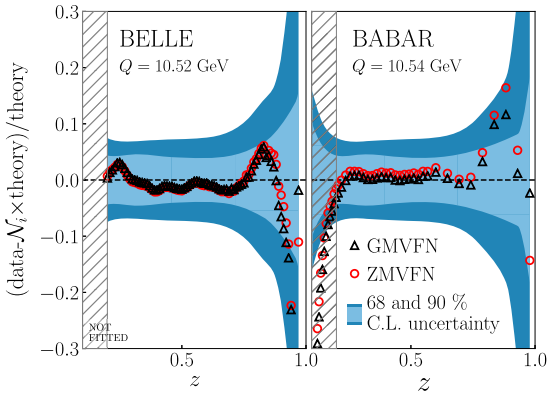

Fig. 2. Comparison between data on normalized single inclusive charged kaon production in electron–positron annihilations from Belle and BaBar and the estimates from the ZMVFN and GMVFN schemes as a function of the kaon energy fraction z. In the case of the comparison to BaBar there is an extra 10% shift applied to the theory estimate in addition to the analytical normalization $\mathcal{N}_i$. The bands represent the uncertainty estimates for the 68 and 90% confidence level limits, for the GMVFN analysis estimated with the improved Hessian approach.

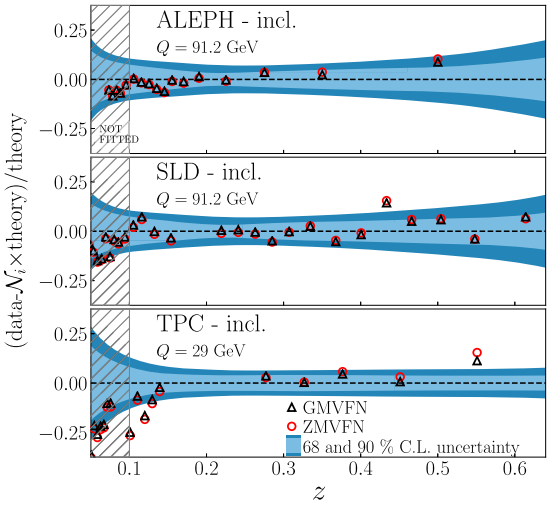

Fig. 3. The same as in Fig. 2 but for ALEPH, SLD and TPC data obtained at higher energy scale.

Figs. 2 and 3 show the degree of agreement between SIA data sets at different energy scales and theory in both the GMVFN and the ZMVFN schemes. It is worth noticing that the improvement in the quality of the fit is not limited to the lower energy scale experiments but has an overall effect. Indeed, higher energy scale data sets, like ALEPH, DELPHI and SLD measurements, are also better described by the GMVFN scheme. As in Ref. [15] we include uncertainty estimates for the 68 and 90 % confidence level limits, estimated with the improved Hessian approach.

The resulting FFs are presented in Fig. 4 as a function of the momentum fraction z for two different energy scales. As a consequence of the introduction of heavy quark mass effects, charm fragmentation probabilities are noticeably modified. The differences are larger than the numerical uncertainty bands computed with a 68% C.L., for most of the z values range, and are preserved at high energy scales by the evolution equations. It can be noticed that no significant differences are found for the light quark FFs. For these particular flavors, the hadronization probabilities are constrained mainly by light flavor tagged SIA and SIDIS data. Most of the high energy flavor tagged SIA data were acquired at the Z-boson mass energy scale, for which charm and bottom quark mass dependent corrections become negligible. On the other hand,

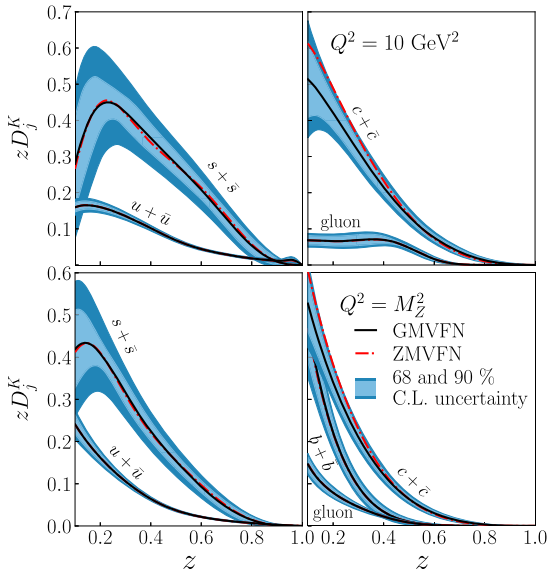

Fig. 4. Parton to kaon FFs as a function of the kaon energy fraction z at $Q^2 = 10$ GeV^2 and $Q^2 = M_Z^2$ coming from the GMVFN (solid black lines) and ZMVFN schemes (dot-dashed lines). The bands represent the uncertainty estimates for the 68 and 90% confidence level limits, for the GMVFN analysis estimated with the improved Hessian approach.

Belle and BaBar constrain very little the bottom hadronization probabilities because of the suppression of its contributions to the SIA single kaon production in both the ZMVFN and the GMVFN schemes. As it shown in Fig. 4, the bottom FF obtained from the inclusion of massive effects differs very little with the massless picture result. Notice that at variance with what happens in the case of the pion FFs [11], the inclusion of the quark mass effects produces a reduction in the charm into kaon FF, whereas for pions quark mass corrections have the opposite effect. The difference can be traced back to the phase space integration of the mass dependent coefficients that produce the above mentioned final effect in the scheme transformation (Eqs. (3)–(6) in Ref. [11]). This dependence of the scheme transformation, prevents anticipating the relevance and specific consequences of the mass effects before the actual extraction is performed and emphasize the usefulness of the analysis presented here.

Going back to the flavor share in the SIA cross section shown in Fig. 1, but now computed with FFs extracted in GNVFN scheme, we can see to what extent the factorization of mass effects into the ZMVFN scheme fragmentation functions leads to an inaccurate picture. As it can be noticed, there is a sizable difference between the estimates of the charm flavor role predicted by the ZMVFN and GMVFN schemes. Even though the charm FF in the ZMVFN is typically larger than the GMVFN one for $z < 0.5$ (Fig. 4), the latter convoluted with the corresponding GMVFN partonic cross section leads to a larger contribution to the SIA cross section (Fig. 1). For $z > 0.5$ the GMVFN charm FF is comparable or larger than the ZMVFN charm FF (Fig. 4) that convoluted with the GMVFN partonic cross section leads to an even larger effect in the SIA cross section. As a consequence, the light flavor contribution estimated in the massless parton approximation are larger than the one obtained with a more consistent description of the heavy quarks dynamics. The difference between both schemes is more conspicuous as larger is the kaon energy fraction. The opposite is true for the charm contribution what implies that the charm contribution to SIA is typically underestimated in the massless framework. Notice that for very large hadron energy fractions ($z > 0.8$) one expects large logarithmic corrections, which appear in each order of perturbation theory, to become increasingly relevant. It is known how to resum such terms to all orders in the strong coupling [31], and it might be worthwhile to explore their relevance in detail in a future dedicated analysis and whether they could further improve the agreement with data. For the moment, we restrict ourselves to the analysis of mass effects, as a first step and for simplicity, in order to avoid the superposition of effects of different origin that certainly could obscure the analysis. In any case, the mass effects are found to be relevant for kaon energy fractions for which resumption effects are expected to be mild. Finally, there is almost no difference between the massless and the massive subtracted predictions for the bottom quark contribution, respectively. Since the most important constraints to the bottom hadronization probabilities are provided by the highest energy data sets, bottom FFs extracted with both schemes are practically identical, and the difference between the partonic cross sections computed through the implementation of the GMVFN and the ZMVFN schemes is suppressed by the convolution with the both small respective FFs.

4. Conclusions

An extension of the GMVFN scheme to extract NLO FFs of quarks and gluons into kaons has been presented. Even though heavy quark mass effects put in evidence by this scheme are comparatively moderate, they already make a difference with present data and will certainly be required to match the precision of the future generation of hadroproduction experiments. The GMVFN framework induces a different energy scale dependence for the heavy quark contribution to the SIA cross section, together with a considerable suppression of these flavors near their mass thresholds. These features lead to inaccurate estimates of the relative importance between light and heavy flavor contributions to the e^+e^- – production of kaons. Specifically, light flavor contribution computed with the ZMVFN is typically larger than the GMVFN results. The differences are more noticeable when the final state kaons carry a larger fraction of the total available energy. This increase is balanced by the charm contribution, which shows the opposite behavior.

References

[1] B.B. Abelev, et al., ALICE Collaboration, Eur. Phys. J. C 73 (12) (2013) 2662.
[2] G. Agakishiev, et al., STAR Collaboration, Phys. Rev. Lett. 108 (2012) 072302.
[3] J.C. Collins, D.E. Soper, G.F. Sterman, Adv. Ser. Dir. High Energy Phys. 5 (1989) 1.
[4] R.P. Feynman, Photon–Hadron Interactions, Reading, 1972.
[5] See, e.g., J. Butterworth, et al., J. Phys. G 43 (2016) 023001.
[6] See, e.g., A. Metz, A. Vossen, Prog. Part. Nucl. Phys. 91 (2016) 136.
[7] M.A.G. Aivazis, J.C. Collins, F.I. Olness, W.K. Tung, Phys. Rev. D 50 (1994) 3102;
R.S. Thorne, R.G. Roberts, Eur. Phys. J. C 19 (2001) 339;
R.S. Thorne, Phys. Rev. D 73 (2006) 054019;
M. Guzzi, P.M. Nadolsky, H.L. Lai, C.-P. Yuan, Phys. Rev. D 86 (2012) 053005.
[8] M. Cacciari, P. Nason, C. Oleari, J. High Energy Phys. 0510 (2005) 034;
T. Kneesch, B.A. Kniehl, G. Kramer, I. Schienbein, Nucl. Phys. B 799 (2008) 34;
B.A. Kniehl, G. Kramer, I. Schienbein, H. Spiesberger, Phys. Rev. D 77 (2008) 014011.
[9] S. Forte, E. Laenen, P. Nason, J. Rojo, Nucl. Phys. B 834 (2010) 116.
[10] R.D. Ball, et al., Phys. Lett. B 754 (2016) 49.
[11] M. Epele, C.A. Garcia Canal, R. Sassot, Phys. Rev. D 94 (3) (2016) 034037.
[12] D. de Florian, R. Sassot, M. Epele, R.J. Hernández-Pinto, M. Stratmann, Phys. Rev. D 91 (1) (2015) 014035.
[13] S. Kretzer, Phys. Rev. D 62 (2000) 054001;
S. Albino, B.A. Kniehl, G. Kramer, Nucl. Phys. B 725 (2005) 181;
S. Albino, B.A. Kniehl, G. Kramer, Nucl. Phys. B 803 (2008) 42;
M. Hirai, S. Kumano, T.-H. Nagai, K. Sudoh, Phys. Rev. D 75 (2007) 094009.
[14] D. de Florian, R. Sassot, M. Stratmann, Phys. Rev. D 75 (2007) 114010.
[15] D. de Florian, M. Epele, R.J. Hernandez-Pinto, R. Sassot, M. Stratmann, Phys. Rev. D 95 (9) (2017) 094019.
[16] J.P. Lees, et al., BaBar Collaboration, Phys. Rev. D 88 (2013) 032011.
[17] M. Leitgab, et al., Belle Collaboration, Phys. Rev. Lett. 111 (2013) 062002.

[18] G. Altarelli, G. Parisi, Nucl. Phys. B 126 (1977) 298;
Y.L. Dokshitzer, Sov. Phys. JETP 46 (1977) 641, Zh. Eksp. Teor. Fiz. 73 (1977) 1216;
V.N. Gribov, L.N. Lipatov, Sov. J. Nucl. Phys. 15 (1972) 438.
[19] M. Stratmann, W. Vogelsang, Phys. Rev. D 64 (2001) 114007.
[20] R.D. Ball, et al., NNPDF Collaboration, J. High Energy Phys. 1504 (2015) 040.
[21] D. Buskulic, et al., Aleph Collaboration, Z. Phys. C 66 (1995) 355.
[22] P. Abreu, et al., Delphi Collaboration, Eur. Phys. J. C 5 (1998) 585.
[23] K. Abe, et al., Sld Collaboration, Phys. Rev. D 59 (1999) 052001.
[24] H. Aihara, et al., Tpc/Two Gamma Collaboration, Phys. Lett. B 184 (1987) 299;
H. Aihara, et al., Tpc/Two Gamma Collaboration, Phys. Rev. Lett. 61 (1988) 1263;
X.-Q. Lu, Ph.D. thesis, Johns Hopkins University, 1987, UMI-87-07273;
W. Braunschweig, et al., TASSO Collaboration, Z. Phys. C 42 (1989) 189.
[25] C. Adolph, et al., COMPASS Collaboration, Phys. Lett. B 767 (2017) 133.
[26] A. Airapetian, et al., Hermes Collaboration, Phys. Rev. D 87 (2013) 074029.
[27] G. Agakishiev, et al., Star Collaboration, Phys. Rev. Lett. 108 (2012) 072302.
[28] B. Abelev, et al., Alice Collaboration, Phys. Lett. B 736 (2014) 196.
[29] I. Borsa, R. Sassot, M. Stratmann, Phys. Rev. D 96 (9) (2017) 094020.
[30] R. Sassot, P. Zurita, M. Stratmann, Phys. Rev. D 82 (2010) 074011.
[31] M. Cacciari, S. Catani, Nucl. Phys. B 617 (2001) 253;
J. Blumlein, V. Ravindran, Phys. Lett. B 640 (2006) 40;
S. Moch, A. Vogt, Phys. Lett. B 680 (2009) 239;
D.P. Anderle, F. Ringer, W. Vogelsang, Phys. Rev. D 87 (2013) 034014.